Dynamic System Response of Truss Panels under High Dynamic Loading through Experimental & Computation Evaluation

Tyrone L. Jones [(i)], Rahul Gupta [(i)], Matthew Burkins [(i)], Haydn Wadley [(ii)] and Yellapu Murty [(iii)]

[i] U.S. Army Research Laboratory (ARL), Aberdeen Proving Ground, MD 21005-5066
[ii] Professor, Department of Materials Science & Engineering, University of Virginia, Charlottesville
[iii] Director, Research and Development, Cellular Materials International, Inc. (CMI)

The ability of computer simulations to accurately resolve dynamic responses of systems has significantly improved over the last decade. Simulations can now be a trusted source of parametric evaluation of complex systems.

DARPA funded a program to investigate the dynamic performance of truss panel systems. Two configurations were computer simulated and their material responses were characterized. This manuscript documents the validity of computer simulation to correlate experimental system failure limits under dynamic load. The computer code matched the experimental outcome in system failure response and residual velocity under high impact. The code can be used in the future to analyze more complex geometries.

1.1 Introduction

Historically, experimental evaluation was the only trusted metric of dynamic performance of system. Computer codes were too inaccurate in their ability to resolve the failure response of multiple materials.

The increasing computational power has simplified the experimental analysis of dynamic impact simulations. Simulations not only reduce the cost and time of manufacturing prototypes, they also provide intimate details of the manner in which a dynamic system responds. The combination of verified computer simulation to experimental data can bound the dynamic limits a system without location inaccuracy.

Simple geometric configurations were evaluated to show how well the computational simulation correlated to the experimental evaluation under high dynamic loading.

1.2 Technology Review

Sandwich panel plays an important role in structures because of its high flexural stiffness-to-weight ratio compared to monocoque and other architectures. It offers lower lateral deformation, higher buckling resistance and higher natural frequency. For a given set of mechanical parameters; sandwich panels often provide lower structural weight compared to monocoque and other architectures.

Even with these advantages, it is desirable to develop means by which to optimize the sandwich construction in order to: (1) compare one sandwich construction with another; (2) compare the best sandwich construction with alternative structural configurations (monocoque, rib-reinforced etc.); (3) select the best face sheet and core materials to minimize structural weight; (4) select the best stacking sequence for face sheets composed of laminated composite materials; (5) compare the optimum structural weight to weights required when there are restrictions (weight penalty due to restrictions of cost, manufacturability etc.) and (6) determine the absolute minimum weight for a given structural geometry, loading and boundary conditions.

The primary purpose of the sandwich core is to insure the spacing between the face sheets and to carry the transverse shear loads to which the structure is subjected. Generally the core comprise of a small percentage of the sandwich weight.

The best way to visualize the structure of a sandwich core panel is to use the analogy of a simple I beam. (Figure 1). A sandwich core

Report Documentation Page

Form Approved
OMB No. 0704-0188

1. REPORT DATE	2. REPORT TYPE	3. DATES COVERED
DEC 2008	**N/A**	**-**

4. TITLE AND SUBTITLE	5a. CONTRACT NUMBER
Dynamic System Response of Truss Panels under High Dynamic Loading through Experimental & Computation Evaluation	5b. GRANT NUMBER
	5c. PROGRAM ELEMENT NUMBER
6. AUTHOR(S)	5d. PROJECT NUMBER
	5e. TASK NUMBER
	5f. WORK UNIT NUMBER
7. PERFORMING ORGANIZATION NAME(S) AND ADDRESS(ES) **U.S. Army Research Laboratory (ARL), Aberdeen Proving Ground, MD 21005-5066**	8. PERFORMING ORGANIZATION REPORT NUMBER
9. SPONSORING/MONITORING AGENCY NAME(S) AND ADDRESS(ES)	10. SPONSOR/MONITOR'S ACRONYM(S)
	11. SPONSOR/MONITOR'S REPORT NUMBER(S)

12. DISTRIBUTION/AVAILABILITY STATEMENT
Approved for public release, distribution unlimited

13. SUPPLEMENTARY NOTES
See also ADM002187. Proceedings of the Army Science Conference (26th) Held in Orlando, Florida on 1-4 December 2008, The original document contains color images.

14. ABSTRACT

15. SUBJECT TERMS

16. SECURITY CLASSIFICATION OF:			17. LIMITATION OF ABSTRACT	18. NUMBER OF PAGES	19a. NAME OF RESPONSIBLE PERSON
a. REPORT	b. ABSTRACT	c. THIS PAGE			
unclassified	**unclassified**	**unclassified**	**UU**	**9**	

panel consists of strong face sheets (flanges) bonded to a core (web), similar to the I beam. The face sheets are subject to tension/compression and are largely responsible for the strength of the sandwich. The function of the core is to support the thin face sheets so that they don't buckle and stay fixed relative to each other. The core experiences mostly shear stress as well as vertical tension and compression. Its material properties and thickness determine the stiffness of such a panel.

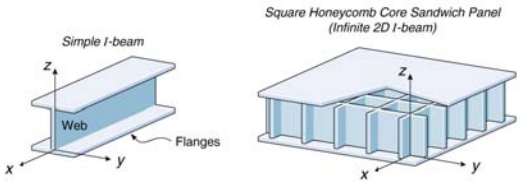

Figure 1: Simple I beam vs. infinite I-beams

Unlike the simple beam which is designed to withstand stresses mostly along the x axis and bending about the y axis, the sandwich panel can be stressed along and about any axis lying in the x-y plane. These panels can extend infinitely; forming a strong and continuous self-sustaining shell (Figure 2).

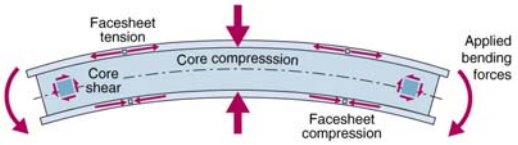

Figure 2: Sandwich panel under bending

Figure 3 illustrates the shear in a weak core. The face sheets experience very little stress because the core deforms easily (low shear modulus of elasticity).

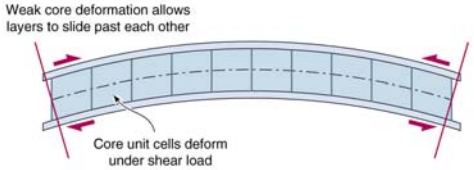

Figure 3: Sandwich panel under bending (weak core)

Figure 4 illustrates the shear in a strong core. The core and face sheets are forced to stretch and compress. Face sheets made of material of high modulus of elasticity work best when used in conjunction with cores of high shear modulus. This balance is important so that neither material fails long before the other is stressed to acceptable level.

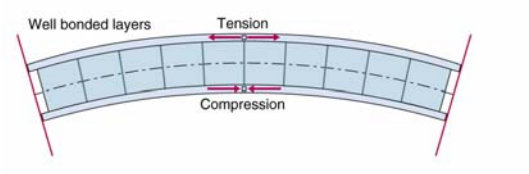

Figure 4: Sandwich panel under bending (strong core)

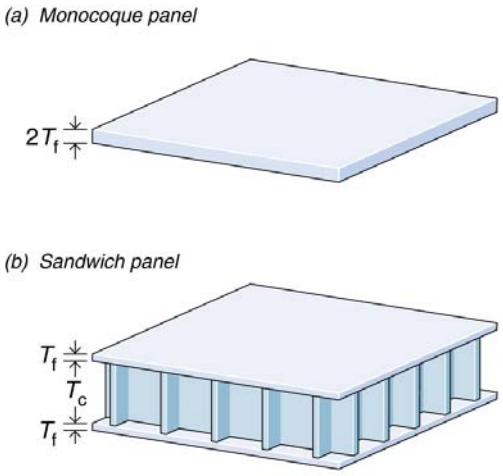

Figure 5: (a) Monocoque plate, (b) Sandwich panel

Let's compare an isotropic sandwich construction with a thin-walled monocoque construction of the same weight. The sandwich construction comprises of two identical face sheets of thickness T_f and a core depth T_c. The monocoque structure on the left has a thickness $2T_f$ (approximately same weight; core material is weight is much lower compared to face sheets).

For an isotropic face sheet with elastic modulus E_f, the extensional stiffness per unit width, K, for both the sandwich and the monocoque construction is:

$$K = 2E_f T_f /(1-\nu_f^2) \qquad (1)$$

Therefore, for in-plane tensile and compressive (up to buckling) loads the two constructions have the same in-plane stiffness. However, there is a marked difference in the flexural stiffness per

unit width, D. For the panel construction of Figure 5(a) above, the flexural stiffness is

$$D_{monocoque} = \frac{E_f (2T_f)^3}{12(1-\nu_f^2)} = \frac{2E_f T_f^3}{3(1-\nu_f^2)} \qquad (2)$$

The flexural stiffness for the sandwich architecture Figure 5(b) is

$$D_{sandwich} = \frac{E_f T_f T_c^2}{2(1-\nu_f^2)} \qquad (3)$$

(Assumption: core doesn't contribute to the flexural stiffness and $\frac{T_f}{T_c}$ <<1)

Therefore, the ratio of the flexural stiffness of sandwich core to a monocoque construction of approximately the same weight using the same face sheet material is:

$$\frac{D_{sandwich}}{D_{monocoque}} = \frac{3}{4}(\frac{T_c}{T_f})^2 \qquad (4)$$

Therefore, if $\frac{T_f}{T_c}$ = 1/2 then the flexural stiffness of the sandwich panel would be 3 times the flexural stiffness of the monocoque plate of approximately the same weight.

Looking at the stress comparison, for an in plane load F per unit width of the structure, and a bending moment per unit width of the structure, M, the shear stress τ is given by:

$$\tau = \frac{N}{2T_f} \qquad (5)$$

Thus, it can be seen that neither construction provides much advantage in this case.

But, in the case of bending moment, M, the monocoque plate results in maximum stress at the top and the bottom surface:

$$\sigma_{monocoque} = \pm\frac{6M}{(2T_f)^2} = \pm\frac{3M}{2T_f^2} \qquad (6)$$

The bending moment M for the sandwich face is:

$$\sigma_{sandwich} = \pm\frac{M}{T_f T_c} \qquad (7)$$

Therefore the ratio of bending stress in a sandwich face to the maximum stress in a monocoque plate of approximately same weight is:

$$\frac{\sigma_{sandwich}}{\sigma_{monocoque}} = \frac{2T_f}{3T_c} \qquad (8)$$

Therefore, if $\frac{T_f}{T_c}$ = 1/2, the bending stress in a sandwich structure is 1/3 of the monocoque plate of approximately the same weight.

The need to protect structures from the high intensity dynamic loads created by explosions has stimulated a renewed interest in the mechanical response of metallic structures subjected to localized, high rate loading [1,2]. One promising approach utilizes sandwich panel concepts to disperse the mechanical impulse transmitted into structures thereby reducing the pressure applied to a protected structure located behind the panel [1-5]. The key component of this panel is a pyramidal lattice core (PLC) panel. The approach begins with various lattice truss structures configured as the cores of sandwich panel structures. Figure 6 shows examples of periodic lattice structures that can be fabricated using affordable processing technologies from light alloys.

A schematic illustration of the basic concept is shown in Figures 7 - 9. Consider a sandwich panel consisting of a pair of solid metal faces and a cellular metal core that is rigidly supported at the edge and an explosive charge is detonated above the system. Several groups have examined the dynamic response of such a configuration [1-5]. Detailed finite element calculations using fully meshed geometries with square honeycomb, prismatic corrugations and pyramidal truss topologies made from materials defined by their yield strength, strain hardening rate, and strain rate sensitivity have been conducted. These studies indicate a complex dynamic structural response. For near field air blasts, a shock wave propagates from the source of the explosion to the front face and is reflected. The pressure resulting from the shock wave decays with distance (from the explosion source)

and time. When the shock is incident upon a rigid surface, the shock wave front undergoes a reflection. This requires the forward moving air molecules comprising the shock wave to be brought to rest and further compressed inducing a reflected overpressure on the wall which is of higher magnitude than the incident overpressure [6-8]. An impulse is imparted to the front face of the structure causing it to acquire a velocity, Figure 9a. In the acoustic limit, the pressure pulse applied to the sample front face during this process is twice that of the free-field shock (large stand-off distances and for weak explosions). In the near field where non-linear effects are present in the shock front, the pressure reflection coefficient can rise to a value of eight (under an ideal gas assumption). Even larger pressure reflection coefficients result when real gas effects (dissociation and ionization of the air molecules) occur in the free field shock [6, 7]. Deshpande and Fleck [9] refer to this initial phase of the blast shock-structure interaction as Stage I.

For an ideal blast with no delayed (reflected) shock arrivals (ground effect), a front face of mass m_f, will be moving at a velocity, V_1, towards the back face sheet, and will have acquired its full momentum ($m_f V_1$) at the end of stage I. For sandwich panel structures, this front face motion is resisted by compression of the cellular core. A region of dense core is then created at the front face and this propagates at the core plastic wave speed towards the back face (Figure 9b). This plastic wave speed

$$V_p = \sqrt{\frac{E_t}{\bar{\rho}}} \qquad (9)$$

where E_t is the tangent modulus of the material used to make the core structure and $\bar{\rho}$ is its relative density. V_p is typically ~500 m/s for stainless steel alloys subjected to plastic strains of around 10%. It is about a tenth of the elastic wave speed of the structural materials.

The core crushing occurs at a characteristic pressure and this pressure resists the front plate movement and slows the front face motion. For weak explosive shocks, it is possible to arrest the densification front within the core [10]. The pressure that is then transmitted to the support structure is controlled by the dynamic crush strength of cellular material during densification [11]. This crush strength depends on the core relative density, the cell topology and the properties of the cellular structure material [12].

For large, spatially localized shock loadings, the impulse transmitted to the back face sheet can be sufficient to cause an edge supported panel to bend. During this panel bending (Stage III), Figure 9c, further mechanical energy dissipation occurs by a combination of core collapse and core/face sheet stretching. In a well designed system, the restraining forces accompanying this plastic dissipation are sufficient to arrest the motion of the panel before the loads applied to the support structure exceed case objectives, or tearing of the front face plate occurs (Figure 8). It is important to recognize that core crushing continues to play an important role during Stage III because highly crush resistant cores maintain a larger face sheet separation and therefore provides higher panels bend resistance [13].

Efforts to implement these blast shock wave protection concepts require a detailed understanding of the dynamic structural response and core collapse mechanisms, the development of a design science that enables preferred core topologies, core relative densities and core materials to be identified, and manufacturing approaches for the materials/topologies of interest. Recent studies indicate that a square honeycomb topology with the webs aligned perpendicular to the face sheets has the highest crush resistance [14]. The dynamic response of this core to a shock wave has been simulated using the finite element method [14].

Significant quasi-static core strength enhancements can be achieved by constructing such cores from metals with a high yield strength and tangent modulus. This causes web buckling to control the core strength and the critical strength for this buckling mode can increase by increasing the web material's tangent modulus. During dynamic loading, additional core strengthening has been predicted to occur by inertial buckling stabilization and strain rate hardening [14]. Materials with a high strength, tangent modulus and strain hardening rate are best suited for blast wave mitigation. Many austenitic and super austenitic stainless steels have a desirable combination of these properties [15]. Recent cellular manufacturing developments now enable the fabrication of many cellular metal core structures from

stainless steels. These include the fabrication of triangular and square honeycombs [16], prismatic corrugations [17], lattice truss structures with pyramidal, tetrahedral, 3-D Kagome architectures [17, 18], and lattice structures with hollow truss or wire mesh lay-ups [19]. These cellular metal cores can be attached to face sheets using transient liquid phase bonding methods to create sandwich panel structures.

1.3. Technical Challenges

The key component of this panel is a pyramidal lattice core (PLC) panel. The approach begins with various lattice truss structures configured as the cores of sandwich panel structures. Figure 6 shows examples of periodic lattice structures that can be fabricated using affordable processing technologies from light alloys. These fabrication techniques are being extended to composites. The resulting structures have very high structural efficiency; their specific strengths are more than 200% greater equivalent mass honeycomb cored structures.

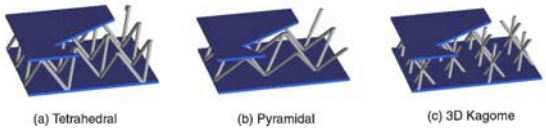

Figure 6. Sandwich panel structures based upon lattice truss cellular topology cores.

Figure 7 shows the characteristics of hollow pyramidal lattices.

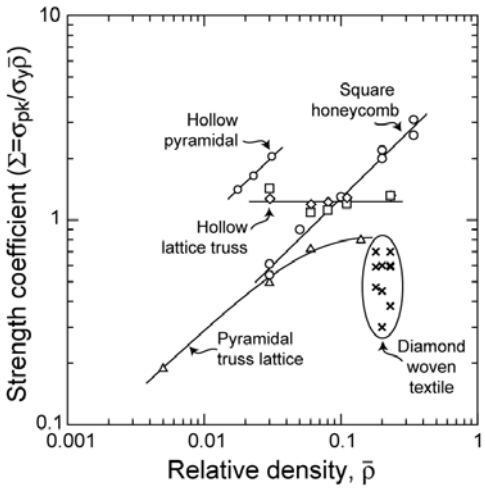

Figure 7. Characteristics of Hollow Pyramidal Lattices

Figure 8 displays the face fracture mechanism.

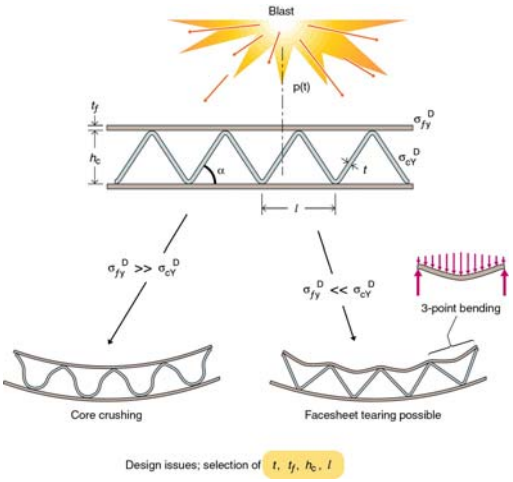

Figure 8. Face Fracture Mechanisms

Figure 9 shows the basic blast mitigation approach. First the blast created shock transfers momentum to the outer face sheet and begins to move towards the back of the structure at a velocity inversely proportional to the mass/unit area of the face sheet. Next, the core begins to crush at the dynamic crush strength (the plateau stress in Figure 9 (b)) and applies retarding forces on the front plate bringing it to rest. The forces transmitted to the back of the structure and the core thickness required to arrest the front face are established by the cellular topology, the core density and the mechanical properties. These structures enable significant mitigation of air borne shocks created by blasts. However, in the form shown in Figure 6, these sandwich panel structures afford only modest levels of ballistic protection. The ARL led team optimized the truss case support structure architecture by adding a ceramic layer to create a structure resistant to blast and projectile impact.

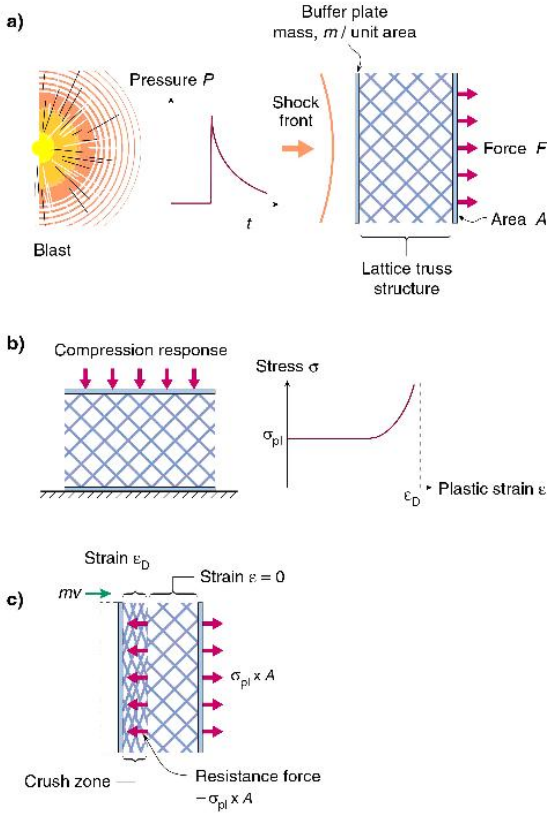

Figure 9. Blast mitigation using cellular metals (core crushing).

Currently, lightweight ceramic composite ballistic panels can be fabricated that provide very good protection against single impacts. However, large clusters of impacts from fragments from IED's collapses the base structure of most composite cases, resulting in large deformations, ceramic damage and delamination of the composite structure. For single impacts, damage to adjacent ceramic tiles and substructure still occurs due to tensile loading of the ceramics from reflected shock waves and localized damage to the backings. 3-D dynamic modeling and simulation of the structure were undertaken at ARL to determine stress distributions for comparison to the penetration and shock evaluation and to optimize the structure. CMI modified the cross-section of the structure based on computational results and testing to reduce weight and cost while maintaining ballistic performance. The result is a robust topological truss core architecture that shows promise for combined protection against blast and projectile impact. The trusses are therefore exceptionally well suited for structural panels such those used for vehicle doors.

2.1 Modeling and Simulation

The goals of the modeling and simulation effort were the following:

- Validate simulations to compare truss core performance against ballistic impacts.
- Determine minimal front face sheet and minimal middle face sheet needed to support ceramic tile under initial ballistic impact.
- Assess dynamic impact behavior of truss structures.

2.2 Material Models

A constitutive model for ceramics by Johnson and Holmquist (which has been validated) is implemented in LS-DYNA. The Johnson-Holmquist Equation of State is referred as *MAT_JOHNSON_HOLMQUIST_CERAMICS . The ceramic layer (SiC) is modeled using this material model. The face sheet / back sheet layers and trusses were modeled with AL_6061 equivalent Johnson Cook material model. The projectile was modeled with RHA equivalent Johnson Cook material model.

3.1 Test Projectile

The 207-grain fragment-simulating projectile (FSP) was used to evaluate the truss plate samples (Figure 10). The 207-grain projectile was produced in accordance with MIL-DTL-46593B (MR), 6 July 2006 [20].

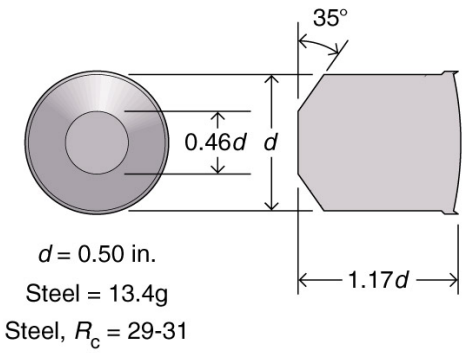

Figure 10. 207 grain projectile

3.2 Analysis summary

The setup and ballistic evaluation of the truss core panels were done in accordance to Military Standard MIL-STD-662F [21]. Figures 11 and 14 display the conversion of the Baseline Case 1 and Case 2, computer-aided design (CAD) solid models to hexahedral finite element analysis (FEA) models respectively. Case 1 (truss core perfectly bonded to a flat tile) was evaluated first. The projectile mushroomed at the ceramic touchdown and the velocity of the projectile at this interface is nil during the initial impact. When the tensile shock wave amplitude is high enough in the ceramic, the ceramic comminutes and the projectile pushes through the ceramic. When the projectile reaches the truss panel, the truss core buckling spreads the load across the face sheets. Figure 12 displays the deformed views of SiC Panel + 6061AL truss core structure for the Baseline Case 1. The simulation correlation was used to prove its ability to successfully optimize the defeat mechanisms and reduce the weight of the case as shown in the deformed views in Figure 13. Case 2 is solved numerically to predict how the result would be for a reverse evaluation of Optimized Case 1. Figure 15 shows the simulation of Case 2.

3.2.1 Baseline Case 1 (Two layer truss core structure): CAD solid model to Hexahedral FEA model, (threat from top) (all dimension units are in inches)

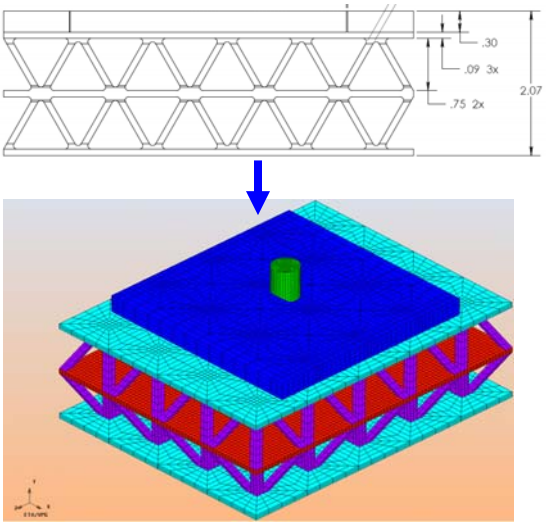

Figure 11. Case 1: Two layer truss core structure (threat from top)

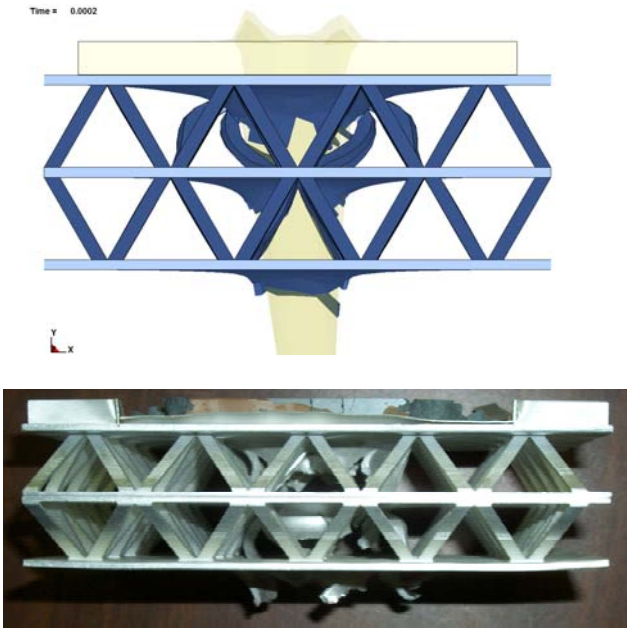

Figure 12. Baseline Case 1: Experimental correlation of deformed views of SiC Panel + 6061AL truss core structure (207-grain projectile impact simulation for 150 μs). V_exit / V_entry = 0.52 (simulation), V_exit / V_entry = 0.41 (experiment), complete penetration (failure) (predicted by simulation and matched by experiment).

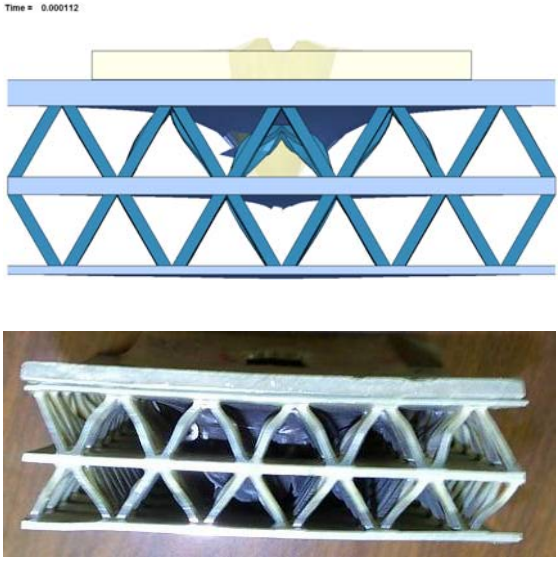

Figure 13. Optimized Case 1: 207-grain projectile impact, V_exit / V_entry = 0.00, partial penetration (success) (predicted by simulation and matched by experiment).

3.2.2 Case 2 (Two layer truss core structure): CAD solid model to Hexahedral FEA model, (identical to Case 1 except threat is from bottom):

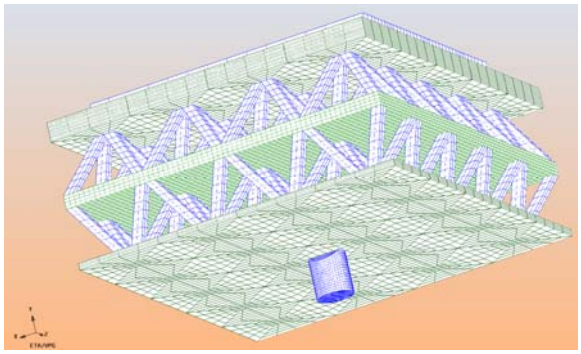

Figure 14. Case 2: Two layer truss core structure (threat from bottom)

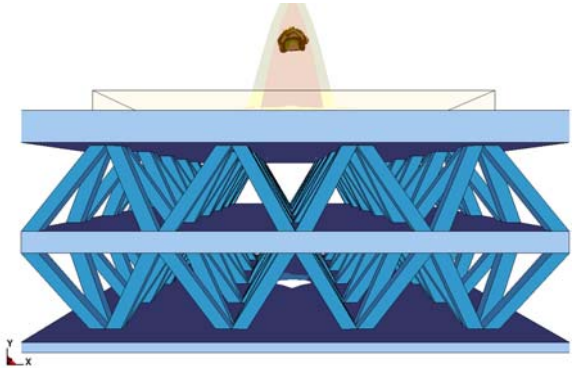

Figure 15. Case 2 (Optimized case 1 with threat reversal): Complete penetration (simulation)

3.2.3 Comparison of Optimized Case 1 and Case 2

The truss core architecture was optimized until the goal of complete stoppage of the 207-grain projectile was achieved. The SiC layer thickness as well as the front / middle face thicknesses was incremented one step at a time until the goal was met. Optimized Case 1 achieved partial penetration (success) while Case 2 (Optimized Case 1 with reverse impact direction) led to complete penetration (failure). This leads us to the conclusion that greater initial neutralization of kinetic energy is achieved at impact with the ceramic material (Case 1) viz a viz metal back plate (Case 2) leading to success in arresting the projectile (confirmed through experiment).

Figure 16 displays the normalized comparative velocity profile plots of the 207-grain projectile.

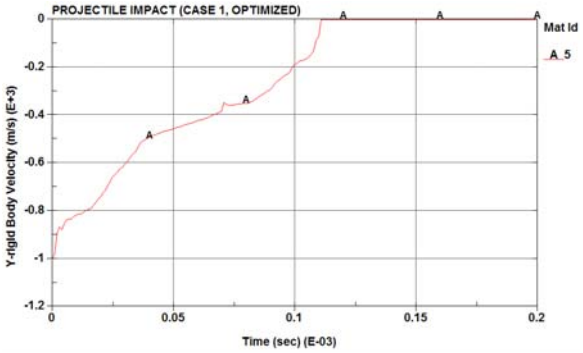

(a)

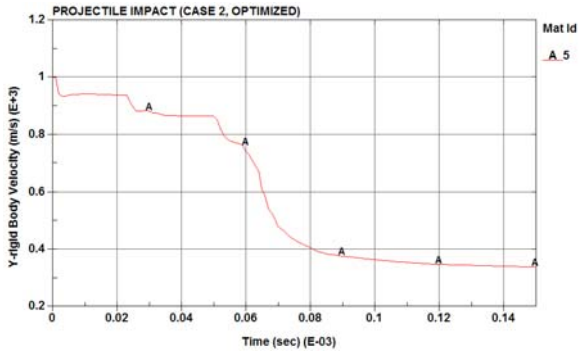

(b)

Figure 16. Velocity / Time histories for Optimized Case 1 and Case 2 (207-grain projectile impact), (a) V_exit / V_entry = 0.00, partial penetration (success) (predicted by simulation and matched by experiment), (b) V_exit / V_entry = 0.34, complete penetration (failure) (predicted by simulation)

4.1 Conclusion and Summary

The simulation showed close correlation with experimental results for both cases. Applying the ceramic to the front spreads the kinetic energy through the truss core during impact (clearly evident in the simulation and the experiment). Reversing the projectile direction failed to decelerate the 207-grain projectile. The code showed robustness in its ability to simulate different panel configurations and offers the ability to simulate more complex truss core architectures in the future.

References

[1]. Fleck NA, Deshpande VS. The resistance of clamped sandwich beams to shock loading. J.Appl. Mech. 2004; 71: 386-401.

[2]. Xue Z, Hutchinson JW. Preliminary assessment of sandwich plates subject to blast loads. Int. J. Mech. Science 2003; 45: 687-705.

[3]. Xue Z, Hutchinson JW. A comparative study of impulse-resistant metal sandwich plates. Int. J. Impact Eng. 2004; 30: 1283-1305.

[4]. Rathbun HJ, Radford DD, Xue Z, He MY, Yang J. Deshpande VS, Fleck NA, Hutchinson JW, Zok FW, Evans AG. Performance of metallic honeycomb-core sandwich beams under shock loading. Int. J. Solids and Structures, submitted 2004.

[5]. Hutchinson JW, Xue Z. Metal Sandwich Plates optimized for pressure impulses, Int. J. Mech. Sci. 2005; 47: 545-569.

[6]. Baker WE, Explosions in Air, University of Texas Press, Austin, TX. (1973).

[7]. Smith PD, Hetherington JG, Blast and Ballistic Loading of Structures, Butterworth-Heinemann, 1994.

[8]. ConWep blast simulation software, U.S. Army Corps of Engineers, Vicksburg, MS.

[9]. Deshpande VS, Fleck NA. Blast resistance of Clamped Sandwich Beams, ICTAM04

[10]. Fleck NA, Deshpande VS. The resistance of clamped sandwich beams to shock loading, J.Appl. Mech. 2004; 71: 386-401.

[11]. Ashby MF, Evans AG, Fleck NA, Gibson LJ, Hutchinson JW, Wadley HNG. Metal Foams: A Design Guide. London: Butterworth-Heinemann; 2000.

[12]. Gibson LJ, Ashby MF. Cellular Solids: Structure and Properties, Cambridge University Press. 2nd edition, 1997.

[13]. Plantema FJ, Sandwich construction, John Wiley and Sons Inc., New York, 1966.

[14]. Xue Z and Hutchinson J., Crush dynamics of square honeycomb sandwich cores, International Journal for Numerical Methods in Engineering, In press, 2005.

[15]. Nemat-Nasser S, Guo WG, and Kihl DP, Thermomechanical response of AL-6XN stainless steel over a wide range of strain rates and temperatures, Journal of the Mechanics and Physics of Solids 2001; 49: 1823-1846.

[16]. Wadley HNG, Fleck NA, Evans AG, Fabrication and structural performance of periodic cellular metal sandwich structures, Composites Science and Technology 2003; 63: 2331-2343.

[17]. Kooistra GW, Deshpande VS, Wadley HNG, Compressible behavior of age hardenable tetrahedral lattice truss structures made from aluminum, Acta Materialia 2004; 52: 4229-4237.

[18]. Wang J, Evans AG, Dharmasena KP, Wadley HNG, On the performance of truss panels with Kagome cores, Int. J. Solids and Structures 2003; 40: 6981-6988.

[19]. Queheillalt DT, Wadley HNG, Cellular metal lattices with hollow trusses, Acta Materialia 2005; 53: 303-313.

[20]. U.S. Army Research Laboratory. *Projectile, Calibers .22, .30, .50, and 20-mm Fragment-Simulating*; Military Specification MIL-DTL-46593B (MR); Aberdeen Proving Ground, MD, 06 July 2006.

[21] Military Standard MIL-STD-662F. V50 *Ballistic Test for Armor*, U.S. Army Research Laboratory: Aberdeen Proving Ground, MD, 18 December 1997.